HHS Public Access

Author manuscript

Biochemistry. Author manuscript; available in PMC 2019 April 15.

Published in final edited form as:

Biochemistry. 2018 March 20; 57(11): 1814–1820. doi:10.1021/acs.biochem.7b01271.

Dual Inhibitor of *Staphylococcus aureus* Virulence and Biofilm Attenuates Expression of Major Toxins and Adhesins

Barbara Hofbauer[#†], **Jan Vomacka**[#†], **Matthias Stahl**[†], **Vadim S. Korotkov**[†], **Megan C. Jennings**[‡], **William M. Wuest**[‡,#], and **Stephan A. Sieber**[*,†]

[†]Department of Chemistry, Chair of Organic Chemistry II, Center for Integrated Protein Science (CIPSM), Institute of Advanced Studies (IAS), Technische Universität München (TUM), Lichtenbergstraße 4, D-85747 Garching, Germany

[‡]Department of Chemistry, Temple University, 1910 North 13th Street, Philadelphia, Pennsylvania 19122, United States

[#] These authors contributed equally to this work.

Abstract

Staphylococcus aureus is a major bacterial pathogen that invades and damages host tissue by the expression of devastating toxins. We here performed a phenotypic screen of 35 molecules that were structurally inspired by previous hydroxyamide-based *S. aureus* virulence inhibitors compiled from commercial sources or designed and synthesized de novo. One of the most potent compounds, **AV73**, not only reduced hemolytic alpha-hemolysin production in *S. aureus* but also impeded in vitro biofilm formation. The effect of **AV73** on bacterial proteomes and extracellular protein levels was analyzed by quantitative proteomics and revealed a significant down-regulation of major virulence and biofilm promoting proteins. To elucidate the mode of action of **AV73**, target identification was performed using affinity-based protein profiling (AfBPP), where among others YidC was identified as a target.

Graphical Abstract

[*]**Corresponding Author** stephan.sieber@tum.de.

[#]**Present Address**Prof. William M. Wuest, Department of Chemistry, Emory University, 1515 Dickey Dr. Atlanta, Georgia 30322 USA.

ASSOCIATED CONTENT

Supporting Information

The Supporting Information is available free of charge on the http://ACS_Publications_website at DOI: 10.1021/acs.bio-chem.7b01271.

SI figures and tables, screening compound library, biochemical procedures and syntheses (PDF)

All MS Data, background binders (XLSX)

Notes

The authors declare no competing financial interest.

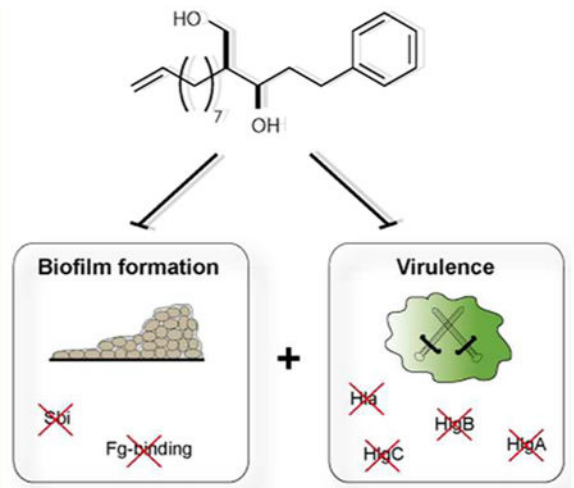

Pathogenic bacteria exploit versatile strategies to infiltrate, hide, grow, and persist within the human body. These processes are promoted by an elaborate arsenal of virulence factors that mediate adherence to host cells, overrun the human immune response, produce toxins, and propagate the formation of biofilms which largely persist antibiotic treatment.[1,2] Given the increasing incidence of untreatable multiresistant bacterial strains and the lack of effective antibiotic therapies, there is a high medical need to identify novel treatment strategies together with chemical entities bearing an unprecedented mode of action. Targeting bacterial virulence, i.e., the production of harmful toxins, has been recently introduced as an alternative route to combat bacterial pathogenesis.[2,3] For example, alpha-hemolysin (Hla) is an erythrocyte lysing toxin and one of the major virulence factors in *S. aureus.* Inhibition of virulence pathways disarms bacteria without directly affecting their viability, thereby not providing a selective pressure and slowing resistance development.[4–8] In addition, bacteria express proteins to facilitate adherence to eukaryotic host cells or initiate attachment to surfaces for the formation of biofilms.[9] The switch from protected biofilms to virulence is tightly controlled to avoid premature elimination of small bacterial populations by the immune response. Thus, pathogenic bacteria such as *Staphylococcus aureus* sense their population density by the production of small autoinducing peptides (AIPs), a process termed quorum sensing (QS), and initiate virulence attack only if a certain quorum is reached.[10,11] QS is regulated by the accessory gene regulator (agr) system encoding membrane bound sensors which turn off biofilm formation and activate virulence gene transcription upon binding of a threshold AIP concentration.[10,12] This antithetic principle is called a double selector switch (DSS) and controlled by RNAIII and Rot.[13]

The most successful attempts to prevent virulence and biofilms are small molecules that mimic AIPs and homoserine lactones and thereby inhibit QS.[14–16] Moreover, biofilms have been recently eradicated by positively charged molecules or cyclic pillararenes.[17–20]

We previously utilized QS independent antivirulence strategies to block caseinolytic protease P (ClpP), a regulator of bacterial virulence, resulting in a global attenuation of toxin expression.[21,22] In our search for optimized antivirulence compounds, we recently identified hydroxyamide fatty acids as potent and durable inhibitors of hla expression.[23] The most

potent hydroxyamide compound **AV59** was effective in an abscess mouse model and did not reveal any in vitro resistance development. A mode of action analysis by affinity-based protein profiling (AfBPP) with an alkyne tagged photo-crosslinker derivative of **AV59** unraveled several target proteins including MntC, an essential component of manganese transport and confirmed antivirulence target.

Inspired by the success of previous antivirulence approaches, we compiled a library of 35 derivatives with diverse structural features. A screen of these molecules against *S. aureus* hemolytic activity revealed a potent inhibitor that even prevented biofilm formation. A closer inspection of the molecular mode of action by quantitative proteomics revealed significant down-regulation of several virulence proteins as well as fibrinogen-binding protein, a mediator of biofilm formation. AfBPP indicated multiple binding partners involved in diverse cellular functions.

MATERIALS AND METHODS

S. aureus Strains and Media.

Commercially available strains were obtained from the following suppliers: Institute Pasteur, France (NCTC8325); American Type Culture Collection (ATCC33591, ATCC6538). Strains SH1000 and USA300–0114 were obtained from Prof. Bettina Buttaro at the Lewis Katz School of Medicine at Temple University. Bacterial growth media: B-medium (LB-Broth 20.0 g/L (Yeast extracts 5.0 g/L, Tryptic peptone 10.0 g/L, NaCl 5.0 g/L), K_2HPO_4 1.0 g/L); BHB-medium (Brain Heart Infusion 17.5 g/L, Na_2HPO_4 2.5 g/L, Glucose 2 g/L, Tryptic peptone 5 g/L, NaCl 5 g/L).

Hemolysis Assay.

5 mL of B-medium was inoculated with 50 μL ON culture and incubated by shaking at 37 °C (200 rpm). After 1.5–2.5 h the culture reached an OD_{600} between 0.4 and 0.6. Bacteria were serially diluted in B-medium (1:9 (v/ v) in 3 steps) to achieve a final concentration of 3.4×10^4 bacteria per mL. For hemolysis assay experiments diluted bacterial cultures were aliquoted into plastic culture tubes (1 mL in each tube) and DMSO (10 μL) or compound in DMSO (10 μL) was added. Bacterial cultures were grown in culture tubes with tightly closed lids at 200 rpm for 20 h at 37 °C. Bacteria were pelleted for 10 min at 6200 × *g* and 100 μL of the supernatant was transferred to a microtiter plate (in triplicate per culture). Next, the supernatant was incubated with 50 μL of diluted sheep blood solution (10% (v/v) in PBS, heparinized sheep blood washed 5× in PBS, Elocin-lab GmbH, Germany) and measured in a 1 min interval at 600 nm, at 37 °C with a plate reader (TECAN, Infinite M200pro). Incubation of 100 μL growth medium with 50 μL diluted sheep blood solution (10% (v/v) in PBS) was used as a negative control. Bacterial supernatant from DMSO control samples (no inhibition of hemolysis) with 50 ^L diluted sheep blood solution was used as a positive control. For the evaluation of IC_{50} values of **AV73** and **AV73-p** the OD_{600} values at 84 min were recorded.

Biofilm Assay.

50 μL of an overnight culture of *S. aureus* NCTC8325 (different procedure for other strains, see Supporting Information) was grown in 5 mL BHB medium in a plastic culture tube. After 1:100 dilution of the culture with fresh BHB medium, test compound in DMSO or DMSO control were added with a volume ratio of 1:100 and the cultures were grown under static conditions at 37 °C for 24 h in a 96-well plate with 100 μL culture per well. Bacterial culture was removed carefully with a multichannel pipet to prevent biofilm destruction. The biofilm was carefully washed with 200 μL ddH_2O. The 96-well plates were dried for 3 h at 37 °C under static conditions and then dried overnight at RT. Per well 50 μL of a 1:5 dilution of 1% (w/v) crystal violet (dissolved in 25% ethanol in ddH_2O) in PBS were added and the plate was incubated for 10 min at RT. The crystal violet solution was removed, the colored biofilm washed 2–4 times with ddH_2O and dissolved in 30% acetic acid in ddH_2O. After 1:10 dilution in 30% acetic acid in ddH_2O absorbance at 595 nm was measured to examine biofilm production.

Mode of Action Analysis.

Whole proteome studies were performed under hemolysis and under biofilm growth conditions using quantitative dimethyl-labeling. AfBPP experiments were done under biofilm conditions with a label-free quantification method. Samples for both methods were analyzed via HPLC-MS/MS using an UltiMate 3000 nano HPLC system (Dionex, Sunnyvale, California, USA) coupled to Thermo Fischer LTQ Orbitrap Fusion (Thermo Fisher Scientific Inc., Waltham, Massachusetts, USA). Peptide and protein identifications were performed using MaxQuant (1.5.3.8. and 1.6.0.1), statistical analysis was done with Perseus 1.6.0.0.

Detailed experimental descriptions to all biochemical experiments and syntheses are provided in the Supporting Information.

RESULTS AND DISCUSSION

Phenotypic Screen for Virulence Inhibitors.

Given the precedence of hydroxyamides as *S. aureus* and MRSA virulence inhibitors, we expanded their structural diversity and compiled a library of 35 compounds with different substitutions. Moreover, **AV59** and previously established derivatives were included as positive controls.[23] Details of the synthetic procedures are provided in the SI. In brief, acids and amides were synthesized from β-lactones, as described previously.[23] The diol, **AV73**, was synthesized by the reduction of the corresponding β-lactone (Scheme S1).

All compounds were initially screened at a concentration of 50 μM against *S. aureus* NCTC8325 hemolysis of sheep erythrocytes in 96-well format (Figure S1). Interestingly, eight compounds showed a drastic reduction of hemolysis and a closer inspection of the hits revealed **AV73, 212, 213,** and **232** as most potent molecules. For example, **AV73** (Figure 1A) reduced hemolytic activity by about 80% at 50 μM concentration and exhibited an EC_{50} of 30 μM (±1.2 μM) (Figure 1B,C). Incubation of the virulence factor containing *S. aureus* secretion medium with **AV73** revealed that Hla function was not directly affected by the

compound (Figure S2). Furthermore, **AV73** did not directly cause lysis of erythrocytes up to a concentration of 1000 μM (Figure S3). As **AV73** was easily accessible for probe synthesis and did not inhibit bacterial growth (>100 μM, data not shown) we selected it for further in depth mechanistic analysis.

Global Down-Regulation of Virulence by AV73.

In order to dissect the antivirulence mode of action we performed a quantitative full-proteome analysis of **AV73** treated and untreated *S. aureus* cells under hemolysis assay conditions. Cells were grown in the presence and the absence of inhibitor, lysed, and digested, and then the peptides were modified with either light or heavy dimethyl isotopes.[24] The samples were pooled, and peptides were separated by liquid chromatography and analyzed via tandem mass spectrometry (LC-MS/MS). Peak ratios of heavy to light labeled peptides were determined and visualized in a volcano plot. Protein hits with an enrichment ($\log_2$ *t* test difference) > 2 were selected for further analysis.

As expected, Hla, the toxin responsible for erythrocyte lysis, belonged to the most down-regulated proteins under hemolysis assay conditions in the soluble fraction confirming results of the phenotypic screen (Figure 1D). Moreover, known effectors of *S. aureus* virulence including transcriptional regulator SarS as well as the two component histidine kinase SaeS were significantly reduced in expression as well.

Since proteins relevant for virulence are often secreted, we analyzed the supernatant of **AV73** treated and untreated bacteria. Importantly, besides Hla, several additional virulence factors including gamma-hemolysin and fibrinogen-binding protein were down-regulated (Figure 1E). A more detailed bioinformatics analysis based on gene ontology (GO) annotation confirmed pathogenesis and cytolysis as significantly down-regulated terms (Table S1).

Fibrinogen-binding protein is crucial for the adherence of *S. aureus* to human cells and hence for the propagation of infections.[25] Moreover, it is essential for the formation of biofilms and the down-regulation observed upon **AV73** treatment opens an intriguing perspective of putative antibiofilm effects.[9]

AV73 is a Potent Inhibitor of Bacterial Biofilms.

To elucidate a putative link to *S. aureus* biofilm we first investigated the **AV73'**s effect on preventing its formation. A single concentration of 50 μM was effective to fully abolish biofilm formation (Figure 2A). Concentration dependent experiments in *S. aureus* strain SH1000, a biofilm forming reference strain, furthermore established a minimal biofilm IC_{50} ($MBIC_{50}$) of 25 μM (Figure 2B). Furthermore, the compound was also effective against other strains including MRSA strain USA300 with an $MBIC_{50}$ of 50 μM, highlighting **AV73** as a promising antibiofilm compound (Figure S4A).

Quantitative proteome analysis of *S. aureus* cells cultivated under biofilm forming conditions in the presence and absence of **AV73** again revealed the down-regulation of major virulence factors and transcriptional regulators including Hla, capsular polysaccharide synthesis (CPS) enzyme and leukocidin like proteins (Figure 2C). A GO enrichment analysis

of extracellular proteins confirmed cytolysis as a down-regulated annotation which became even more evident by the secretome analysis (Table S2). Here, alpha- and gamma-hemolysin, several proteases SplA-F as well as fibrinogen-binding protein were significantly reduced in expression confirming a global antivirulence mode of action that also affected biofilm formation (Figure 2D). To reveal mechanistic insights, we performed target identification via chemical proteomics.

Target Analysis via Affinity-Based Protein Profiling.

Target analysis was performed by affinity-based protein profiling (AfBPP).[26–28] AfBPP traps the reversible binding between ligand and protein by a photo-cross-linker upon UV irradiation *in situ*. AfBPP does not only require a photoreactive group, it also needs the incorporation of an enrichment tag, e.g., an alkyne for click chemistry,[29,30] to pull out the labeled proteins via conjugation to an affinity handle such as biotin. We rationalized that introduction of an azide moiety in the benzene ring in the *para*-position would yield an aryl-azide photo-crosslinker without major structural perturbations. The alkyne handle was incorporated by replacement with the **AV73'**s terminal alkene. Synthesis of this compound followed six steps and was initiated by undec-10-ynoic acid. After TMS protection of the alkyne, thioester formation, and following ketene acetal formation, the lactone was synthesized in a tandem Mukaiyama aldol-lactonization.[31] The lactone was reduced and during azide introduction, the protecting groups were removed to gain **AV73-p** (Scheme 1).

With the probe in hand, we first validated its potency in biofilm and hemolysis inhibition. Antibiofilm and antihemolytic activities were largely retained with IC_{50} values of 30 μM (**AV73:** 25 μM) and 35 μM (**AV73:** 30 μM), respectively, indicating that probe functionalization only minimally affected its biological activity (Figure 1C, Figure 2B, Figure S4B). For target identification, intact *S. aureus* cells, grown under biofilm conditions, were incubated with the probe or DMSO as control, irradiated with UV-light (280–315 nm), lysed, and clicked to either rhodamine- or biotin-azide for target visualization and identification, respectively. Initial studies via fluorescent SDS-PAGE revealed the labeling of several bands with an optimal concentration of 60 (Figure S5). Next, studies were performed via enrichment of probe-biotin labeled proteins on avidin beads, tryptic digestion and analysis via LC-MS/MS with label-free quantification.[32] To account for photocross-linker background binding two controls, competition with **AV73** and labeling with a minimal phenylazide probe, were performed (Figure S6).[33] Enriched proteins as well as their competition with **AV73** and background binders are visualized in corresponding volcano plots (Figure 3A,B, Figure S7, Supporting Excel file). In total six and 13 enriched protein hits could be identified in soluble and insoluble fractions, respectively, bearing an at least 1.5-fold increased enrichment compared to the minimal probe.

Membrane protein insertase YidC, iron compound ABC transporter, sortase, and diadenylate cyclase were among the competed hits (Figure S7C,D). YidC is a crucial integral membrane protein responsible for inserting a diverse set of proteins into the lipid bilayer of bacteria.[34,35] Although no direct evidence for its role in virulence and biofilm formation exists in *S. aureus,* a previous study of two YidC paralogues in *Streptococcus mutans* showed a stress sensitive phenotype as well as impaired biofilm formation upon genetic mutation of

YidC2.[36,37] An additional target, the putative iron compound ABC transporter, lacks firm functional characterization. However, an impact of iron transport is supported by whole proteome data showing the up-regulation of two hemin importers, in response to compound addition (Figure 2C). Moreover, the identified sortase resembles a SrtA-type enzyme anchoring proteins to the extracellular membrane. SrtA additionally cleaves its substrates after threonine in C-terminal LPXTG motifs. Indeed, virulence- and biofilm-associated proteins identified in the **AV73** treated *S. aureus* proteome contain this motif (Table S3).[38,39] Also diadenylate cyclase fits to the observed **AV73** phenotype by the production of cyclic di-AMP, an important transmitter in virulence regulation.[40,41] Overall the identified targets support an **AV73** induced effect on virulence and biofilm formation.

Taken together, our target analysis via AfBPP indicates that **AV73** acts via parallel binding to several proteins associated with pathogenesis matching the antivirulence and antibiofilm phenotype. With stringent controls, we could narrow down the mode of action to four main hits playing yet not fully clarified roles in virulence and biofilm formation. Although this study cannot fully consolidate the mode of action by the identified targets, the whole proteome profiling upon addition of **AV73** points toward a mechanism interfering with virulence regulation via sortase and cyclic di-AMP-mediated signal transduction.

CONCLUSIONS

Given the simplicity of the **AV73** structure, its antibiofilm activity and low toxicity further applications, e.g., as coating, can be envisaged. Of note, the simultaneous downregulation of virulence as well as biofilm related proteins is a major distinction compared to previous studies with lactone inhibitors of the ClpXP proteolytic system that affected solely the Rot/RNAIII regulatory path.[23] Thus, **AV73** acts via a different target pathway that was elucidated here.

Supplementary Material

Refer to Web version on PubMed Central for supplementary material.

ACKNOWLEDGMENTS

We thank Prof. Bettina Buttaro for *S. aureus* strains SH1000 and USA300–0114 and Mona Wolff and Katja Bauml for excellent technical support.

Funding

The work was funded by the Center for Integrated Protein Science Munich (CIPSM) and by the Federal Ministry of Education, Research, Germany, FKZ: 031A131, National Science Foundation (CHE1755698), and the National Institutes of Health (DE025837, GM119426). M.S. was supported by the German Academic Scholarship Foundation. M.C.J. acknowledges a National Science Foundation predoc-toral grant (DGE-1144462).

ABBREVIATIONS

AfBPP	affinity-based protein profiling
agr	accessory gene regulator

AIPs	autoinducing peptides
ClpP	caseinolytic protease P
CPS	capsular polysaccharide synthesis
DSS	double selector switch
GO	gene ontology
Hla	alpha-hemolysin
QS	quorum sensing

REFERENCES

(1). Zecconi A, and Scali F (2013) Staphylococcus aureus virulence factors in evasion from innate immune defenses in human and animal diseases. Immunol. Lett. 150, 12–22. [PubMed: 23376548]

(2). Ruer S, Pinotsis N, Steadman D, Waksman G, and Remaut H (2015) Virulence-targeted Antibacterials: Concept, Promise, and Susceptibility to Resistance Mechanisms. Chem. Biol. Drug Des. 86, 379–399. [PubMed: 25589217]

(3). Clatworthy AE, Pierson E, and Hung DT (2007) Targeting virulence: a new paradigm for antimicrobial therapy. Nat. Chem. Biol. 3, 541–548. [PubMed: 17710100]

(4). Hung DT, Shakhnovich EA, Pierson E, and Mekalanos JJ (2005) Small-molecule inhibitor of Vibrio cholerae virulence and intestinal colonization. Science 310, 670–674. [PubMed: 16223984]

(5). Rasko DA, Moreira CG, Li de R, Reading NC, Ritchie JM, Waldor MK, Williams N, Taussig R, Wei S, Roth M, Hughes DT, Huntley JF, Fina MW, Falck JR, and Sperandio V (2008) Targeting QseC signaling and virulence for antibiotic development. Science 321, 1078–1080. [PubMed: 18719281]

(6). Khodaverdian V, Pesho M, Truitt B, Bollinger L, Patel P, Nithianantham S, Yu G, Delaney E, Jankowsky E, and Shoham M (2013) Discovery of antivirulence agents against methicillin-resistant Staphylococcus aureus. Antimicrob. Agents Chemother. 57, 3645–3652. [PubMed: 23689713]

(7). Tang F, Li WH, Zhou X, Liu YH, Li Z, Tang YS, Kou X, Wang SD, Bao M, Qu LD, Li M, and Li B (2014) Puerarin protects against Staphylococcus aureus-induced injury of human alveolar epithelial A549 cells via downregulating alpha-hemolysin secretion. Microb. Drug Resist. 20, 357–363. [PubMed: 24372183]

(8). Allen RC, Popat R, Diggle SP, and Brown SP (2014) Targeting virulence: can we make evolution-proof drugs? Nat. Rev. Microbiol. 12, 300–308. [PubMed: 24625893]

(9). Hall-Stoodley L, Costerton JW, and Stoodley P (2004) Bacterial biofilms: from the natural environment to infectious diseases. Nat. Rev. Microbiol. 2, 95–108. [PubMed: 15040259]

(10). George EA, and Muir TW (2007) Molecular mechanisms of agr quorum sensing in virulent staphylococci. ChemBioChem 8, 847–855. [PubMed: 17457814]

(11). Waters CM, and Bassler BL (2005) Quorum sensing: cell- to-cell communication in bacteria. Annu. Rev. Cell Dev. Biol. 21, 319–346. [PubMed: 16212498]

(12). Frees D, Sorensen K, and Ingmer H (2005) Global virulence regulation in Staphylococcus aureus: pinpointing the roles of ClpP and ClpX in the sar/agr regulatory network. Infect. Immun. 73, 8100–8108. [PubMed: 16299304]

(13). Nitzan M, Fechter P, Peer A, Altuvia Y, Bronesky D, Vandenesch F, Romby P, Biham O, and Margalit H (2015) A defense-offense multi-layered regulatory switch in a pathogenic bacterium. Nucleic Acids Res. 43, 1357–1369. [PubMed: 25628364]

(14). Tal-Gan Y, Stacy DM, Foegen MK, Koenig DW, and Blackwell HE (2013) Highly potent inhibitors ofquorum sensing in Staphylococcus aureus revealed through a systematic synthetic study of the group-III autoinducing peptide. J. Am. Chem. Soc. 135, 7869–7882. [PubMed: 23647400]

(15). Lowery CA, Abe T, Park J, Eubanks LM, Sawada D, Kaufmann GF, and Janda KD (2009) Revisiting AI-2 quorum sensing inhibitors: direct comparison of alkyl-DPD analogues and a natural product fimbrolide. J. Am. Chem. Soc. 131, 15584–15585. [PubMed: 19824634]

(16). Opoku-Temeng C, and Sintim HO (2017) Targeting c-di- GMP Signaling, Biofilm Formation, and Bacterial Motility with Small Molecules. Methods Mol Biol. 1657, 419–430. [PubMed: 28889311]

(17). Minbiole KPC, Jennings MC, Ator LE, Black JW, Grenier MC, LaDow JE, Caran KL, Seifert K, and Wuest MW (2016) From antimicrobial activity to mechanism of resistance: the multifaceted role of simple quaternary ammonium compounds in bacterial eradication. Tetrahedron 72, 3559–3566.

(18). Bottcher T, Kolodkin-Gal I, Kolter R, Losick R, and Clardy J (2013) Synthesis and activity of biomimetic biofilm disruptors. J. Am. Chem. Soc. 135, 2927–2930. [PubMed: 23406351]

(19). Jennings MC, Ator LE, Paniak TJ, Minbiole KP, and Wuest WM (2014) Biofilm-eradicating properties of quaternary ammonium amphiphiles: simple mimics of antimicrobial peptides. ChemBioChem 15, 2211–2215. [PubMed: 25147134]

(20). Joseph R, Naugolny A, Feldman M, Herzog IM, Fridman M, and Cohen Y (2016) Cationic Pillararenes Potently Inhibit Biofilm Formation without Affecting Bacterial Growth and Viability. J. Am. Chem. Soc. 138, 754–757. [PubMed: 26745311]

(21). Böttcher T, and Sieber SA (2008) Beta-lactones as specific inhibitors of ClpP attenuate the production of extracellular virulence factors of Staphylococcus aureus. J.Am. Chem. Soc. 130, 14400–14401. [PubMed: 18847196]

(22). Hackl MW, Lakemeyer M, Dahmen M, Glaser M, Pahl A, Lorenz-Baath K, Menzel T, Sievers S, Bottcher T, Antes I, Waldmann H, and Sieber SA (2015) Phenyl Esters Are Potent Inhibitors of Caseinolytic Protease P and Reveal a Stereogenic Switch for Deoligomerization. J. Am. Chem. Soc. 137, 8475–8483. [PubMed: 26083639]

(23). Vomacka J, Korotkov VS, Bauer B, Weinandy F, Kunzmann MH, Krysiak J, Baron O, Bottcher T, Lorenz-Baath K, and Sieber SA (2016) An Aromatic Hydroxyamide Attenuates Multiresistant Staphylococcus aureus Toxin Expression. Chem. - Eur. J. 22, 1622–1630. [PubMed: 26748534]

(24). Boersema PJ, Raijmakers R, Lemeer S, Mohammed S, and Heck AJ (2009) Multiplex peptide stable isotope dimethyl labeling for quantitative proteomics. Nat. Protoc. 4, 484–494. [PubMed: 19300442]

(25). Peacock SJ, Foster TJ, Cameron BJ, and Berendt AR (1999) Bacterial fibronectin-binding proteins and endothelial cell surface fibronectin mediate adherence of Staphylococcus aureus to resting human endothelial cells. Microbiology 145, 3477–3486. [PubMed: 10627045]

(26). Lapinsky DJ, and Johnson DS (2015) Recent developments and applications of clickable photoprobes in medicinal chemistry and chemical biology. Future Med. Chem. 7, 2143–2171. [PubMed: 26511756]

(27). Geurink PP, Prely LM, van der Marel GA, Bischoff R, and Overkleeft HS (2011) Photoaffinity labeling in activity-based protein profiling. Top. Curr. Chem. 324, 85–113.

(28). Evans MJ, and Cravatt BF (2006) Mechanism-based profiling of enzyme families. Chem. Rev. 106, 3279–3301. [PubMed: 16895328]

(29). Tornoe CW, Christensen C, and Meldal M (2002) Peptidotriazoles on Solid Phase: [1,2,3]-Triazoles by Regiospecific Copper(l)-Catalyzed 1,3-Dipolar Cycloadditions of Terminal Alkynes to Azides. J. Org. Chem. 67, 3057–3064. [PubMed: 11975567]

(30). Rostovtsev VV, Green JG, Fokin VV, and Sharpless KB (2002) A stepwise Huisgen cycloaddition process: copper(l)-catalyzed regioselective “ligation” of azides and terminal alkynes. Angew. Chem., Int. Ed. 41, 2596–2599.

(31). Cho SW, and Romo D (2007) Total Synthesis of (–)-Belactosin C and Derivatives via Double Diastereoselective Tandem Mukaiyama Aldol Lactonizations. Org. Lett. 9, 1537–1540. [PubMed: 17378572]

(32). Cox J, Hein MY, Luber CA, Paron I, Nagaraj N, and Mann M (2014) Accurate proteome-wide label-free quantification by delayed normalization and maximal peptide ratio extraction, termed MaxLFQ. Mol. Cell. Proteomics 13, 2513–2526. [PubMed: 24942700]

(33). Kleiner P, Heydenreuter W, Stahl M, Korotkov VS, and Sieber SA (2017) A Whole Proteome Inventory of Background Photocrosslinker Binding. Angew. Chem. Int. Ed. 56, 1396–1401.

(34). Li Z, Boyd D, Reindl M, and Goldberg MB (2014) Identification of YidC residues that define interactions with the Sec Apparatus. J. Bacteriol. 196, 367–377. [PubMed: 24187090]

(35). Xie K, and Dalbey RE (2008) Inserting proteins into the bacterial cytoplasmic membrane using the Sec and YidC translocases. Nat. Rev. Microbiol. 6, 234–244. [PubMed: 18246081]

(36). Palmer SR, Crowley PJ, Oli MW, Ruelf MA, Michalek SM, and Brady LJ (2012) YidC1 and YidC2 are functionally distinct proteins involved in protein secretion, biofilm formation and cariogenicity of Streptococcus mutans. Microbiology 158, 1702–1712. [PubMed: 22504439]

(37). Hasona A, Zuobi-Hasona K, Crowley PJ, Abranches J, Ruelf MA, Bleiweis AS, and Brady LJ (2007) Membrane composition changes and physiological adaptation by Streptococcus mutans signal recognition particle pathway mutants. J. Bacteriol. 189, 1219–1230. [PubMed: 17085548]

(38). Frankel BA, Bentley M, Kruger RG, and McCafferty DG (2004) Vinyl sulfones: inhibitors of SrtA, a transpeptidase required for cell wall protein anchoring and virulence in Staphylococcus aureus. J. Am. Chem. Soc. 126, 3404–3405. [PubMed: 15025450]

(39). Novick RP (2000) Sortase: the surface protein anchoring transpeptidase and the LPXTG motif. Trends Microbiol. 8, 148–151. [PubMed: 10754567]

(40). Opoku-Temeng C, Dayal N, Miller J, and Sintim HO (2017) Hydroxybenzylidene-indolinones, c-di-AMP synthase inhib¬itors, have antibacterial and anti-biofilm activities and also re-sensitize resistant[space]bacteria to methicillin and vancomycin. RSC Adv. 7, 8288–8294.

(41). Gries CM, Bruger EL, Moormeier DE, Scherr TD, Waters CM, and Kielian T (2016) Cyclic di-AMP Released from Staphylococcus aureus Biofilm Induces a Macrophage Type I Interferon Response. Infect. Immun. 84, 3564–3574. [PubMed: 27736778]

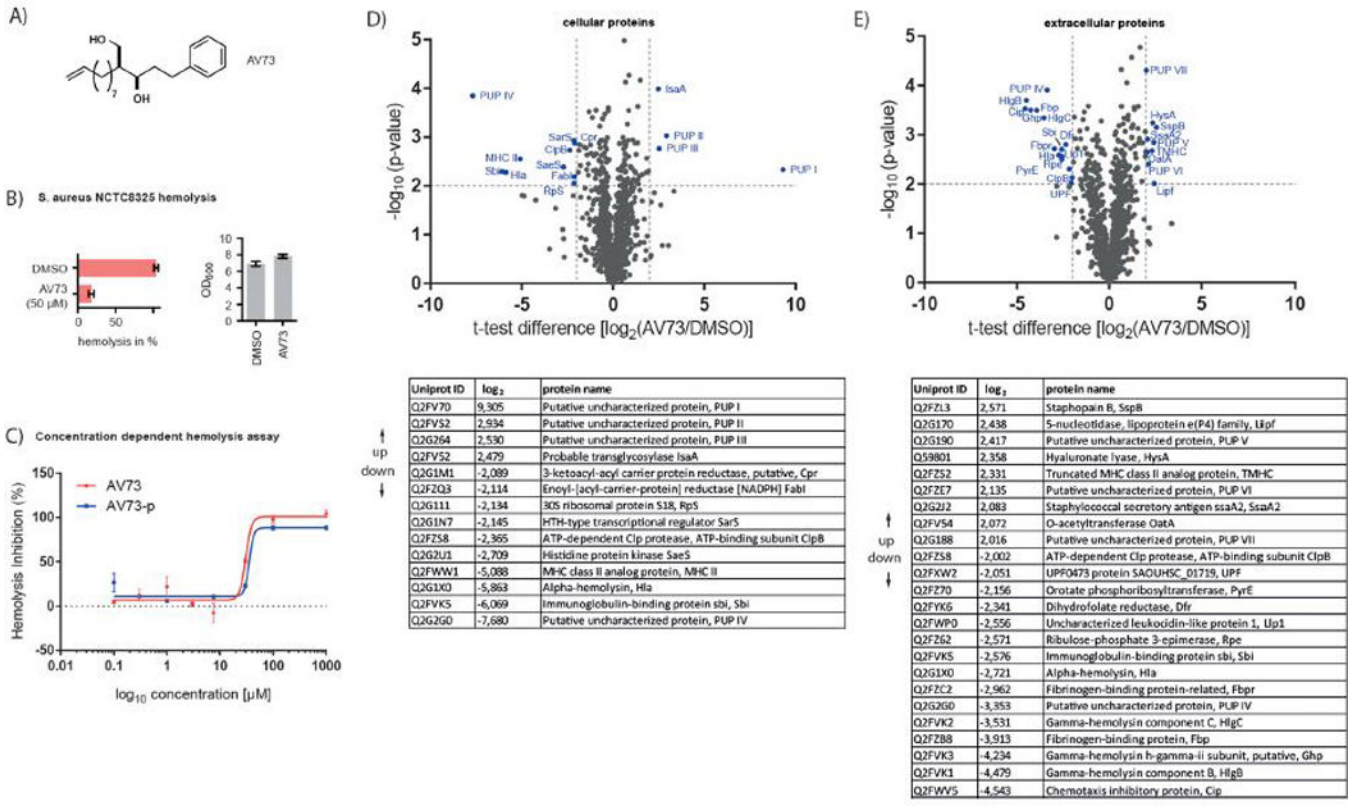

Uniprot ID	log2	protein name
Q2FV70	9,305	Putative uncharacterized protein, PUP I
Q2FV52	2,934	Putative uncharacterized protein, PUP II
Q2G264	2,530	Putative uncharacterized protein, PUP III
Q2FV52	2,479	Probable transglycosylase IsaA
Q2G1M1	-2,089	3-ketoacyl-acyl carrier protein reductase, putative, Cpr
Q2FZQ3	-2,114	Enoyl-[acyl-carrier-protein] reductase [NADPH] FabI
Q2G111	-2,134	30S ribosomal protein S18, RpS
Q2G1N7	-2,145	HTH-type transcriptional regulator SarS
Q2FZS8	-2,365	ATP-dependent Clp protease, ATP-binding subunit ClpB
Q2G2U1	-2,709	Histidine protein kinase SaeS
Q2FWW1	-5,088	MHC class II analog protein, MHC II
Q2G1X0	-5,863	Alpha-hemolysin, Hla
Q2FVK5	-6,069	Immunoglobulin-binding protein sbi, Sbi
Q2G2G0	-7,680	Putative uncharacterized protein, PUP IV

Uniprot ID	log2	protein name
Q2FZL3	2,571	Staphopain B, SspB
Q2G170	2,438	5-nucleotidase, lipoprotein e(P4) family, Llpf
Q2G190	2,417	Putative uncharacterized protein, PUP V
Q59801	2,358	Hyaluronate lyase, HysA
Q2FZS2	2,331	Truncated MHC class II analog protein, TMHC
Q2FZE7	2,135	Putative uncharacterized protein, PUP VI
Q2G2J2	2,083	Staphylococcal secretory antigen ssaA2, SsaA2
Q2FV54	2,072	O-acetyltransferase OatA
Q2G188	2,016	Putative uncharacterized protein, PUP VII
Q2FZS8	-2,002	ATP-dependent Clp protease, ATP-binding subunit ClpB
Q2FXW2	-2,051	UPF0473 protein SAOUHSC_01719, UPF
Q2FZ70	-2,156	Orotate phosphoribosyltransferase, PyrE
Q2FYK6	-2,341	Dihydrofolate reductase, Dfr
Q2FWP0	-2,556	Uncharacterized leukocidin-like protein 1, Llp1
Q2FZ62	-2,571	Ribulose-phosphate 3-epimerase, Rpe
Q2FVK5	-2,576	Immunoglobulin-binding protein sbi, Sbi
Q2G1X0	-2,721	Alpha-hemolysin, Hla
Q2FZC2	-2,962	Fibrinogen-binding protein-related, Fbpr
Q2G2G0	-3,353	Putative uncharacterized protein, PUP IV
Q2FVK2	-3,531	Gamma-hemolysin component C, HlgC
Q2FZB8	-3,913	Fibrinogen-binding protein, Fbp
Q2FVK3	-4,234	Gamma-hemolysin h-gamma-ii subunit, putative, Ghp
Q2FVK1	-4,479	Gamma-hemolysin component B, HlgB
Q2FWV5	-4,543	Chemotaxis inhibitory protein, Cip

Figure 1.

(A) Structure of **AV73.** (B) Hemolysis assay of **AV73** at 50 μM and DMSO in *S. aureus* NCTC8325. The assay was performed with a suspension of sheep erythrocytes in PBS added to bacterial supernatants. The time-resolved decrease in OD_{600} was measured. (C) Concentration dependent hemolysis assay of **AV73** and **AV73-p** in *S. aureus* NCTC8325 in three biological replicates. EC_{50} (**AV73**) = 30 μM (±1.2 μM), EC_{50} (**AV73-p**) = 35 μM (±5.0 μM). (D) Whole proteome analysis of cellular proteins, performed under hemolysis conditions in four biological replicates. Most regulated proteins are marked and sorted in decreasing *t* test difference order. Cutoff lines were set at a minimum $\log_2$ fold-change of 2 and a minimum $\log_{10}$ (*p*-value) of 2. (E) Whole proteome analysis of extracellular proteins was performed in four biological replicates. Most regulated proteins are again listed. Cutoff lines were set at a minimum $\log_2$ fold-change of 2 and a minimum $-\log_{10}$ (*p*-value) of 2.

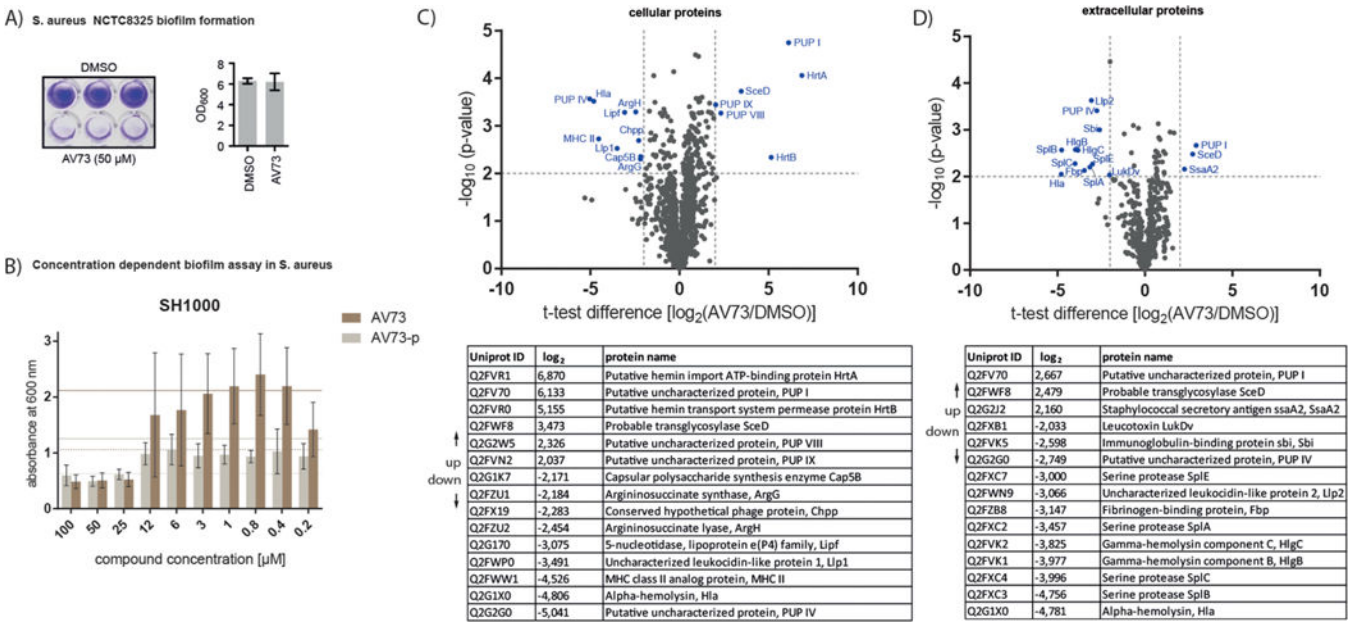

Uniprot ID	log_2	protein name
Q2FVR1	6,870	Putative hemin import ATP-binding protein HrtA
Q2FV70	6,133	Putative uncharacterized protein, PUP I
Q2FVR0	5,155	Putative hemin transport system permease protein HrtB
Q2FWF8	3,473	Probable transglycosylase SceD
Q2G2W5	2,326	Putative uncharacterized protein, PUP VIII
Q2FVN2	2,037	Putative uncharacterized protein, PUP IX
Q2G1K7	-2,171	Capsular polysaccharide synthesis enzyme Cap5B
Q2FZU1	-2,184	Argininosuccinate synthase, ArgG
Q2FX19	-2,283	Conserved hypothetical phage protein, Chpp
Q2FZU2	-2,454	Argininosuccinate lyase, ArgH
Q2G170	-3,075	5-nucleotidase, lipoprotein e(P4) family, Lipf
Q2FWP0	-3,491	Uncharacterized leukocidin-like protein 1, Llp1
Q2FWW1	-4,526	MHC class II analog protein, MHC II
Q2G1X0	-4,806	Alpha-hemolysin, Hla
Q2G2G0	-5,041	Putative uncharacterized protein, PUP IV

up / down

Uniprot ID	log_2	protein name
Q2FV70	2,667	Putative uncharacterized protein, PUP I
Q2FWF8	2,479	Probable transglycosylase SceD
Q2G2J2	2,160	Staphylococcal secretory antigen ssaA2, SsaA2
Q2FXB1	-2,033	Leucotoxin LukDv
Q2FVK5	-2,598	Immunoglobulin-binding protein sbi, Sbi
Q2G2G0	-2,749	Putative uncharacterized protein, PUP IV
Q2FXC7	-3,000	Serine protease SplE
Q2FWN9	-3,066	Uncharacterized leukocidin-like protein 2, Llp2
Q2FZB8	-3,147	Fibrinogen-binding protein, Fbp
Q2FXC2	-3,457	Serine protease SplA
Q2FVK2	-3,825	Gamma-hemolysin component C, HlgC
Q2FVK1	-3,977	Gamma-hemolysin component B, HlgB
Q2FXC4	-3,996	Serine protease SplC
Q2FXC3	-4,756	Serine protease SplB
Q2G1X0	-4,781	Alpha-hemolysin, Hla

up / down

Figure 2.

(A) Biofilm assay of **AV73** at 50 μM and DMSO in *S. aureus* NCTC8325. Biofilms of bacteria were grown under static conditions in 96-well plates and were stained with crystal violet. Bacterial growth with and without **AV73** was determined by OD_{600} measurement. (B) Concentration dependent biofilm assay of **AV73** and **AV73-p** in *S. aureus* SH1000. Solid line represents the DMSO control, the dashed line is half the OD_{600} of the DMSO control. The experiment was performed in three biological replicates. $MBIC_{50}$ (**AV73**) < 25 μM, MBIC50 (**AV73-p**) < 30 μM. The high OD_{600} difference between the two compounds is due to the inconsistent biofilm growth, which especially occurs without inhibition. (C) Whole proteome analysis of cellular proteins, performed under biofilm conditions in four biological replicates. Most significantly regulated proteins are marked and listed after decreasing *t* test difference. Cutoff lines were set aminimum log_2 fold-change of 2 and a minimum $-log_{10}$ (*p*-value) of 2.(D) Whole proteome analysisof extracellular proteins performed in four biological replicates. Most significantly regulated proteins are listed. Cutoff lines were set at a minimum of log2 fold-change of 2 and a minimum $-log_{10}$ (*p*-value) of 2.

A) **AfBPP: soluble fraction**

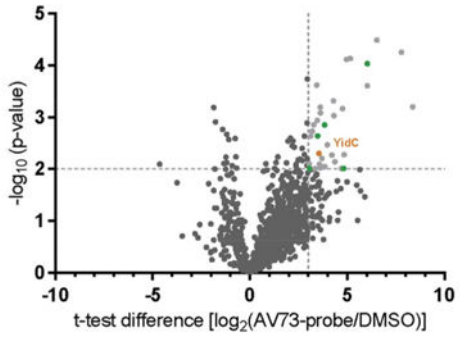

Ratio > |1.5|	Uniprot ID	Protein name
1,86	Q2FWG4	Membrane protein insertase YidC
1,98	Q2FY09	CBS domain protein
2,24	Q2FVQ2	Uncharacterized lipoprotein SAOUHSC_02650
3,80	Q2FZG5	Uncharacterized protein
>100	Q2FV45	Uncharacterized protein
>100	Q2G002	3-dehydroquinate dehydratase

B) **AfBPP: insoluble fraction**

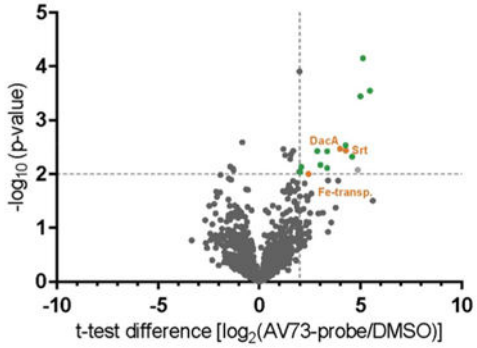

Ratio > |1.5|	Uniprot ID	Protein name
1,52	Q2G2W5	Uncharacterized protein
1,57	Q2G247	UPF0478 protein SAOUHSC_01855
1,62	Q2FW64	Uncharacterized protein
1,85	Q2FWX4	Uncharacterized protein
1,95	Q2G193	Uncharacterized protein
3,10	Q2FV99	Sortase, putative, Srt
3,59	Q2FW92	Diadenylate cyclase, DacA
4,86	Q2G257	Uncharacterized protein
6,53	Q2FWA8	Lytic regulatory protein, putative
7,91	Q2FVQ2	Uncharacterized lipoprotein
8,26	Q2FVN4	Uncharacterized protein
39,39	Q2FXH8	Uncharacterized protein
>100	Q2FWE1	Release factor glutamine methyltransferase

Figure 3.

(A) AfBPP volcano plot of **AV73-p** against DMSO in the soluble fraction. The experiment was performed in four biological replicates. Cutoff lines were set at a minimum of $\log_2$ fold-change of 3 and a minimum $-\log_{10}$ (*p*-value) of 2. Proteins depicted in gray are found equally enriched in the background volcano plot. Green marked proteins are found less enriched in the background volcano plot, as shown in the tables below. The orange marked protein is referred to in the text. (B) Volcano plot of **AV73-p** against DMSO in the insoluble fraction. The experiment was performed in four biological replicates. Cutoff lines were set at

a minimum of $\log_2$ fold-change of 2 and a minimum $-\log_{10}$ (*p*-value) of 2. Color code same as in (A).

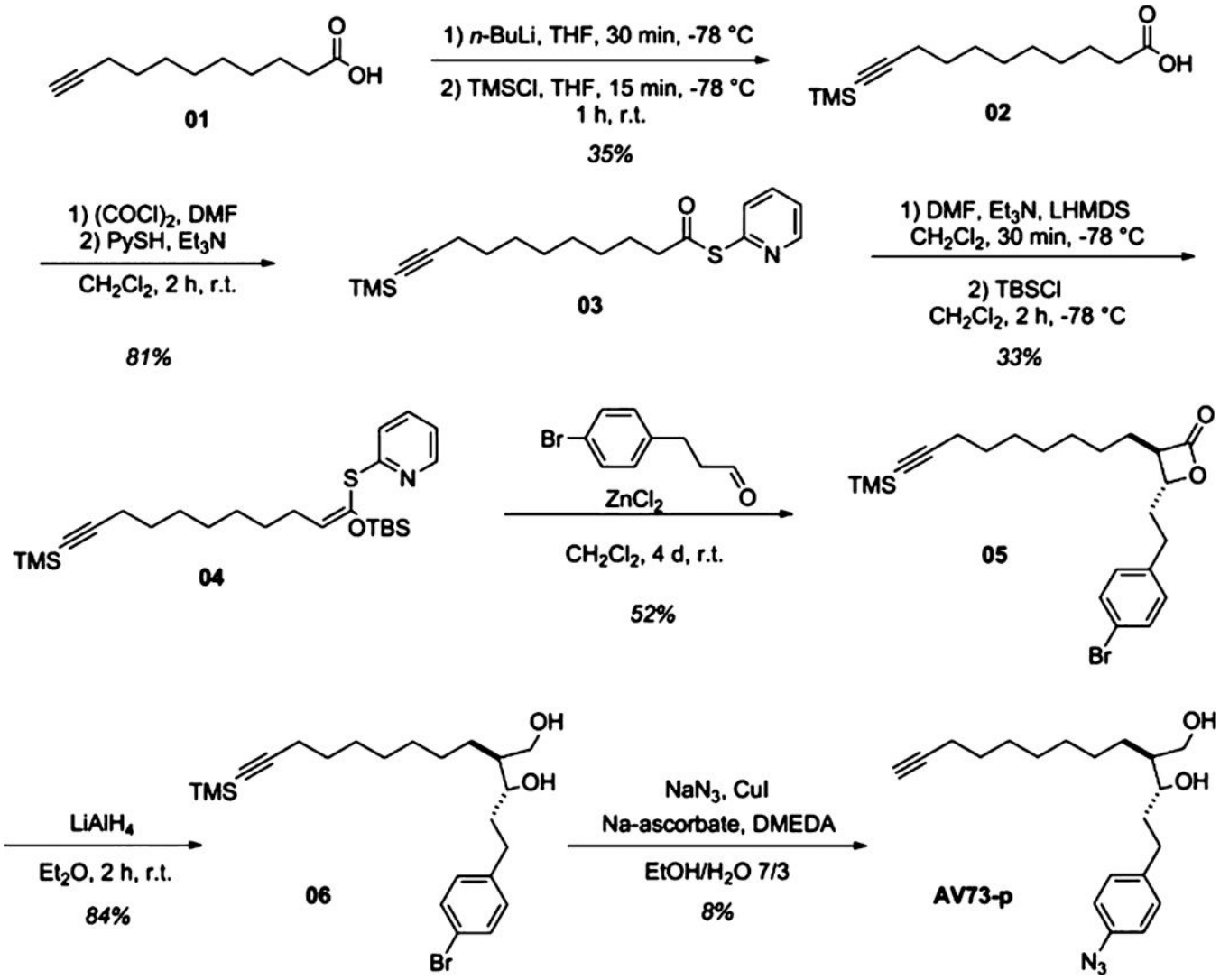

Scheme 1.
Synthesis of the Affinity-Based Protein Profiling (AfBPP) Probe AV73-p